*Article*

# Assessment of Water Resources Availability in Amu Darya River Basin Using GRACE Data

**Obaidullah Salehie** [1,2], **Tarmizi bin Ismail** [1], **Shamsuddin Shahid** [1], **Mohammed Magdy Hamed** [3], **Pennan Chinnasamy** [4] **and Xiaojun Wang** [5,6,*]

[1] Department of Water and Environmental Engineering, School of Civil Engineering, Faculty of Engineering, Universiti Teknologi Malaysia (UTM), Skudia 81310, Johor, Malaysia; salehie1985@graduate.utm.my (O.S.); tarmiziismail@utm.my (T.b.I.); sshahid@utm.my (S.S.)

[2] Faculty of Environment, Kabul University, Kabul 1007, Afghanistan

[3] Construction and Building Engineering Department, College of Engineering and Technology, Arab Academy for Science, Technology and Maritime Transport (AASTMT), B 2401 Smart Village, Giza 12577, Egypt; eng.mohammedhamed@aast.edu

[4] Centre for Technology Alternatives for Rural Areas (CTARA), Indian Institute of Technology Bombay, Mumbai 400076, India; p.chinnasamy@iitb.ac.in

[5] State Key Laboratory of Hydrology–Water Resources and Hydraulic Engineering, Nanjing Hydraulic Research Institute, Nanjing 210029, China

[6] Research Center for Climate Change, Ministry of Water Resources, Nanjing 210029, China

[*] Correspondence: xjwang@nhri.cn

**Abstract:** Water is diminishing in many places of the globe due to human intervention and climate variability. This study was conducted to assess water sustainability in the Amu Darya basin, the largest river catchment of central Asia, using two Gravity Recovery and Climate Experiment (GRACE) satellite solutions with a spatial resolution of $0.5°$. Spatial variability of water sustainability was estimated by integrating reliability, resiliency and vulnerability. In addition, the Modified Mann–Kendall (MMK) test was utilized to detect the significant trends in water availability. Findings show a significant decline in the basin's water supply, especially after 2010. Water availability was more variable in the east and a small area in the south. Trend analysis revealed higher declination in water availability in the range of $-0.04$ to $-0.08$ cm/year in the tundra and warm dry continental climate zones and the delta region of the basin ending in the Aral Sea in the cold desert climate zone. Water resources in the cold semi-arid (steppe) and most parts of the cold desert climate are more sustainable than the rest of the basin. Overall, the results indicate that water resources availability in a large-scale basin with climate diversity could be well assessed using the method used in this study.

**Keywords:** water availability; sustainability index; equivalent water thickness; GRACE; Amu Darya basin

## 1. Introduction

Freshwater is one of the fundamental elements of Earth and the core of sustainable development. It is vital to maintain the ecosystems' functionality, support socioeconomic activities to reduce poverty and improve environmental sustainability to enhance livelihoods [1]. The variability of water resources in space and time has made it insufficient to meet human needs in many parts of the globe [2–4]. Factors limiting water resources availability includes deviations in land use, demography and climate, particularly precipitation and temperature [5–10]. Water engineers and politicians are increasingly concerned about the influence of climate change on water supplies, particularly in arid and semi-arid areas [9,11–13]. It has intensified freshwater competition between sectors globally [14]. However, water scarcity in different regions depends on the capability and infrastructures of the area to handle impact or adapt to alteration [15].

Global water demand has increased by about 1.8% per year in the past 100 years [16]. It is likely to increase by 55% by 2050, mainly due to increasing demand in manufacturing,

hydropower generation and domestic use [1]. Therefore, pressure on the water system will continue to rise with population growth and economic activity [17]. Sustainability in water sources must be well understood, responding to these various water demands to avoid hindrance in economic development and people's livelihood improvement [18].

Any water availability studies should provide information on annual available water and its vulnerability to understand whether the available water sources are sufficient to meet the demand [19]. Spatiotemporal water availability information in a catchment helps monitoring and sustainable water resource management [20]. Insufficient hydrological information causes weak water management and worse water supply for any consumption [21].

Water availability and consumption are closely linked to the broader concept of water sustainability in water resources management [22]. Sustainable water resources management promotes the growth of water resources, maximizes economic utility and enhances social welfare without compromising the integrity and sustainability of the environment [22]. Numerous techniques and models have been established to measure water resources sustainability [23]. Currently, adaptability to changing water resources is the core of attention, which refers to minimizing the vulnerability to present or expected future changes [24]. For example, Loucks [25] suggested a sustainability index for assessing water resource sustainability based on risk criteria. Sandoval-Solis et al. [24] introduced a sustainability index for water resource planning and management by improving the structure, content and scale of an earlier sustainability index to make it more flexible and adaptable to the needs of each water customer, purpose and watershed.

Climate variability and anthropogenic actions have significantly altered water availability [26]. It is important to evaluate the spatial distribution of sustainability in water resources in the changing environment. It needs data on water resources, including surface water, groundwater and soil moisture data. It is also expected that the data should be available at multiple sites distributed over the whole basin. However, it is quite different to obtain such a volume of data in practice, particularly for the basins located in developing regions. Gravity Recovery and Climate Experiment (GRACE) equivalent water thickness (EWT) data provides an estimation of total water held above and below the Earth's surface, such as groundwater, soil moisture storage, surface water storage and snow water equivalent [27,28]. GRACE EWT can be used for spatiotemporal analysis of water resources availability and sustainability [29]. Thus, GRACE helps overcome the abovementioned limitations, and thus, it is widely used globally [30]. GRACE satellite data aim to measure the Earth's gravitational field every 30 days for five years with a resolution of 400 km [31]. This data product is available from 2002 to the present. It is not applicable for local water resource management due to its coarse spatial resolution, but it is suited for such study over large river basins [27,32]. GRACE data were available through the Jet Propulsion Laboratory (JPL), Center for Space Research (CSR) at the University of Texas, Austin, and GeoForschungsZentrum Potsdam (GFZ) [33].

Many researchers used GRACE to evaluate terrestrial water, groundwater, surface water or drought changes. For example, Wang et al. [34] utilized GRACE to detect water storage changes at China's Three Gorges Reservoir. Researchers such as Mo et al. [35] and Shamsudduha et al. [36] analyzed variations in EWT over land and river basins using GRACE or in conjunction with the Global Land Data Assimilation System (GLDAS), while Li et al. [37] used it to assess changes in Australia's Murray-Darling basin groundwater storage. Other researchers used it for hydrological drought assessment and monitoring [38–41].

Central Asian countries, dominated by arid and semi-arid climates, are vulnerable to climate variation and water stress [42,43]. The Amu Darya river is the longest transboundary river in Central Asia (CA); it originates from the headwater of Tien Shan and Pamir and provides support to sustain the livelihoods and economy of most agriculture-dependent populations in CA [44]. It forms about 39% of Afghanistan's territory, while 61% of the river flows within other countries [45,46]. The Amu Darya, which flows through Afghanistan, Kyrgyzstan, Tajikistan, Turkmenistan and Uzbekistan, provides water for drinking, agricul-

ture and hydropower and sustains the Aral Sea [47–49]. The river basin is home to about 80 million people [45]. Snow and glacier melted water contributes more river discharge, particularly with peak flow in summer (June to September) in the headwater tributaries Panj and Vakhsh rivers [50,51]. Deserts mostly cover the lower part of the Amu Darya with a mean annual rainfall of only 80 mm, high winds, scorching summers and very cold winters [52].

Glacier retreating in the source region of Amu Darya due to earth warming has been projected by some researchers. This might have an impact on the region's water supply. For example, Lutz et al. [53] projected a reduction of the current glacier extent in the upper Amu Darya basin by nearly 430 km$^2$ in 2050. At the same time, the annual water demand in the basin would increase by 3.8–5.0% [54]. White et al. [55] projected the future climate of the basin for 2070–2099. They showed that 34–49% of the basin's present 3.4 million hectares of irrigated land would dry out in a 1:20 year drought by the end of the century, and runoff is likely to drop by 10–20% of current levels. In contrast, glacier melting would have less contribution to river flow.

As mentioned before, a few studies have been conducted in the Amu Darya basin to project future climate impacts, but no detailed study showed sustainability in water availability. Immerzeel et al. [56] demonstrated that the Amu Darya basin lacks studies using new methods. Therefore, this study was conducted to find terrestrial water supply in the Amu Darya basin using GRACE data and the water resources sustainability. This study also attempted to connect water sustainability with land use and the basin population. The study's findings will help identify water vulnerable regions and adaptation needs.

## 2. Study Area

The Amu Darya river is the longest international river (2540 km) shared by a part of five landlocked CA counties, Afghanistan, Tajikistan, Kyrgyzstan, Turkmenistan and Uzbekistan [51,57,58]. Rising from the headwaters in the snowfields of the high mountains of Tajikistan, Kyrgyzstan, the north of Hindu Kush and Whakhan in Afghanistan, it flows through Karakum and Kyzylkum deserts and ends in the Aral Sea [57,59–62]. It has an average annual flow of 78.5 km3 [63]. Out of the total length of the Amu river, 1250 km are within Afghanistan territory or along its border [64]. Vahsh, Pandj and Zeravshan are the main tributaries to the Amu river [65]. The basin's climate is continental, with chilly winters, scorching summers, little precipitation and low relative humidity. It is too dry to maintain a forest but not extremely dry to become a desert [66]. The Amu river watershed can be classified into five major climatic zones, as shown in Figure 1. It is mainly split into three uneven zones: (1) an upstream characterized by the high-mountain features with a 7495 m altitude; (2) a midstream with several patches of large irrigated oases; and (3) a downstream zone in the northwest with an around 200 m elevation with a delta and feeding the Aral Sea. The maximum precipitation in the upstream (Eastern Pamir) of the Amu Darya is 2000 mm (mean annual of 464 mm), while the downstream mean annual rainfall is below 100 mm. Rainfall occurs from November to May, and summer is hot with an average temperature of 35 °C. Autumn is cool and rainy (18 °C), and winter is cold and snowy with an average temperature of −8 °C to −20 °C [67,68].
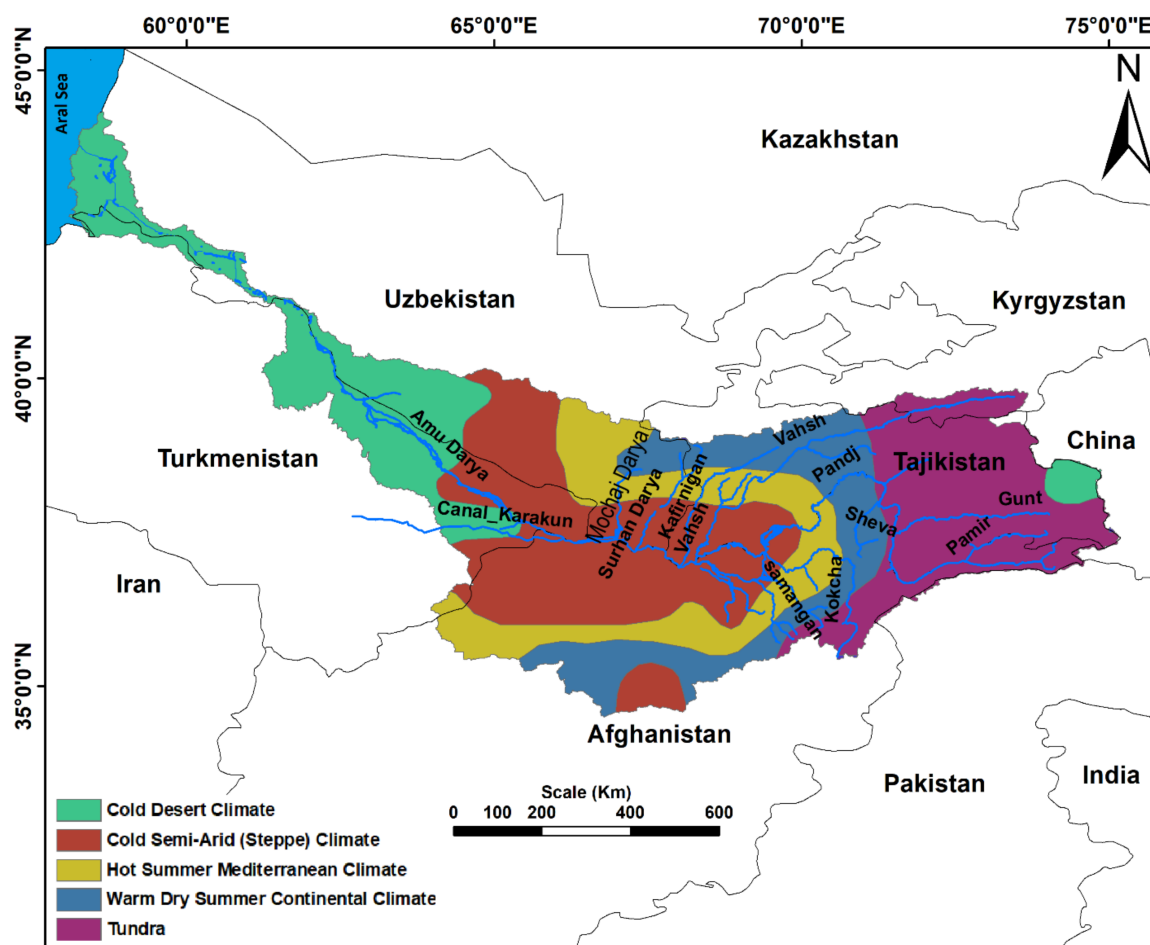
**Figure 1.** The climate zones of the Amu Darya river basin.

## 3. Research Method

The procedure followed in this research is described below:

1.  Two solutions of GRACE datasets (CSR and JPL) with a spatial resolution of 0.5° were extracted for the Amu Darya basin (total 241 grid points).
2.  The above GRACE solutions were used to estimate EWT trend using Sen's slope estimator and modified Mann–Kendall (MMK) tests to assess the spatiotemporal variability of water storage change over the basin.
3.  The water sustainability index was applied to assess water availability in terms of change in EWT reliability, resiliency and vulnerability (RRV) at all grid points over the basin.
4.  The indices were standardized between 0 and 1 to remove the influence of individual indexes.
5.  All the outcomes from RRV were mapped using ArcGIS.

### 3.1. Trend Analysis of Water Availability

Sen's slope estimator was used to estimate EWT changes, and the MMK test was used to determine the significance of trends. Sen's slope is a nonparametric technique used to predict the magnitude of change in climatic time series data. It measures the rate of change between two successive data points (Q):

$$Q_i = \frac{x_i - x_k}{i - k} \text{ for } N = 1, 2, 3, \ldots, n \tag{1}$$

where $x_i$ and $x_k$ are two data points at times i and k. The Sen's estimator of the slope is the median of these n values of $Q_i$ as follows:

$$Q = \begin{cases} \frac{Q_{N+1}}{2} & \text{if N is odd} \\ \frac{1}{2}\left(\frac{Q_N}{2} + \frac{Q_{N+2}}{2}\right) & \text{if N is even} \end{cases} \tag{2}$$

The MK test statistic (S) for a time series $x_1$, $x_2$, $x_3$ ... and $x_n$ can be calculated as follows:

$$S = \sum_{k=1}^{n-1} \sum_{i=k+1}^{n} \text{sign}(x_i - x_k) \tag{3}$$

$$\text{where sign}(x_i - x_k) = \begin{cases} +1 \text{ if sign}(x_i - x_k) > 0 \\ 0 \text{ if sign}(x_i - x_k) = 0 \\ -1 \text{if sign}(x_i - x_k) < 0 \end{cases} \tag{4}$$

where n is the number of data points, $x_k$ and $x_i$ are the time-series observations, and S is the sum of positive or negative signs. The variance of S is used to estimate Z statistic to decide trend significance,

$$Z = \begin{cases} \frac{S-1}{\sqrt{\text{Var (S)}}} & \text{when S} > 0 \\ 0 & \text{when S} = 0 \\ \frac{S+1}{\sqrt{\text{Var (S)}}} & \text{when S} < 0 \end{cases} \tag{5}$$

Z would be positive for the upward trend while negative for the downward trend. The null hypothesis of no trend is rejected at a confidence interval of 95% if $|Z| > 1.96$.

To resolve the problems of autocorrelation in time series data, Hirsch and Slack proposed the MMK trend test [69]. The MMK test is conducted when the null hypothesis of no trend is rejected. The procedure of MMK begins with assessing the trend using the MK test. Thus, if there is a significant trend in the time series, the MMK test de-trends the series and ranks the data (Ri) to estimate its equivalent normal variants (Zi) using the inverse standard normal distribution function ($\varnothing^{-1}$),

$$Z_i = \varnothing^{-1}\left(\frac{R_i}{n+1}\right) \text{ for i} = 1 : n \tag{6}$$

where $\varnothing^{-1}$ is the inverse standard normal distribution function, and n is the length of the time series. The Z is used to calculate the Hurst coefficient (H) through the maximum log-likelihood function [70].

$$\log L(H) = -\frac{1}{2}\log|C_n(H)| - \frac{z^\tau[C_n(H)]^{-1}Z}{2\gamma_0} \tag{7}$$

where $|C_n(H)|$ is the determinant of the correlation matrix of lag for a given H; $z^\tau$ indicates the transpose and variance of Z; the value of H that yields the maximum value of log L(H) is counted to define the presence of long-term dependency in the time series. The significance of H can be attained by using mean and standard deviation for H = 0.5. When H is found to be significant, the biased estimate of $\text{Var}(S)^{H'}$ can be expressed as follows:

$$\text{Var}(S)^{H'} = \sum_{i<j} \cdot \sum_{k<l} \frac{2}{\pi} \sin^{-1}\left(\frac{\rho|j-i| - \rho|i-1| - \rho|j-k| + \rho|i-k|}{\sqrt{(2-2\rho|i-j|)(2-2\rho|k-l|)}}\right) \tag{8}$$

where ρl is the autocorrelation function for a given H.

### 3.2. Assessment of Water Resources Availability

The variation in sustainability in water resources was assessed using the sustainability index proposed by Loucks [25] and modified by Sandoval-Solis et al. [24], which defined sustainability (S) as a function of reliability, resiliency and vulnerability as follows:

$$S = [\text{Reliability} \times \text{Resiliency} \times (1 - \text{Dimensionless Vulnerability})]^{\frac{1}{3}} \qquad (9)$$

The RRV metrics provide an optimal method for evaluating the chance of success or failure of a structure and the rate of recovery of a system from unsatisfactory states [71]. Here, we followed the RRV defined by Hashimoto et al. [72] and Sandoval-Solis et al. [24]. The reliability of EWT describes the frequency of change in EWT and how often it drops below the mean level. The resiliency is expressed as the recovery of EWT to its normal situation after a decline. The vulnerability measures the extent of an event and shows the total water deficit in an event. Dimensionless vulnerability can be obtained by the division of vulnerability over the demand. The reliability, resiliency and dimensionless vulnerability are expressed as follows:

$$\text{Reliability} = 1 - \frac{\sum_{j=1}^{M} d(j)}{T} \qquad (10)$$

$$\text{Resiliency} = \left( \left( \frac{1}{M} \right) \sum_{j=1}^{M} d(j) \right)^{-1} \qquad (11)$$

$$\text{Vulnerability} = \left( \frac{1}{M} \right) \sum_{j=1}^{M} v(j) \qquad (12)$$

$$\text{Dimensionless Vulnerability} = \frac{\left( \frac{1}{M} \right) \sum_{j=1}^{M} v(j)}{\text{Demand}} \qquad (13)$$

In Equations (10)–(13), d(j) indicates the duration of the j-th negative EWT event; M refers to the number of water deficit events, unitless; T is total number of time intervals, minute or hour; and v(j) indicates the value of deficit events (unitless). In the present study, the value of 'Demand' in Equation (13) was considered −1, following Hashimoto et al. [72].

## 4. Results

### 4.1. Monthly Mean Anomaly of EWT

Figure 2 depicts the EWT anomalies of the GRACE data of the CSR and JPL at five different climate zones (Figure 1) of the Amu Darya river basin: (a) cold desert in the northwest of the basin in the territory of Uzbekistan and Turkmenistan; (b) the cold semi-arid (steppe) zone; (c) hot-summer Mediterranean; (d) warm dry summer continental and (e) tundra in the eastern part of the basin for all months during the study period of 2002–2019. The positive anomaly of EWT is presented using blue and negative using red in the figure. The blue color indicates the months when water availability is higher than the mean for the study period and vice versa for the red.

Both solutions show almost similar patterns in seasonal variability of EWT for all climate zones, except in the cold desert climate zone. In the early years, the water availability was above the mean level from February to July and below the mean level during September to December in all the climate zones. Overall, it was above its mean level for a longer period (January to July) in the hot-summer Mediterranean climate zone and fewer months (February to May) in the cold climate zone. In recent years, the EWT gradually declined in all climate zones except in the cold climate zone. For example, it was generally above the mean level in January–July during 2002–2007, but it was above the mean level only in February–April in recent years (2012–2019). In some years, it never reached the mean level, particularly in hot-summer Mediterranean, warm dry summer continental and tundra climate zones (Figure 2c–e). An opposite scenario was noticed for the cold desert

climate zone (Figure 2a). Water has become more available in recent years in the region. Though the results of the two products were not consistent for this climate zone, both GRACE products showed a reduction of red color in recent years, indicating an increase in EWT.
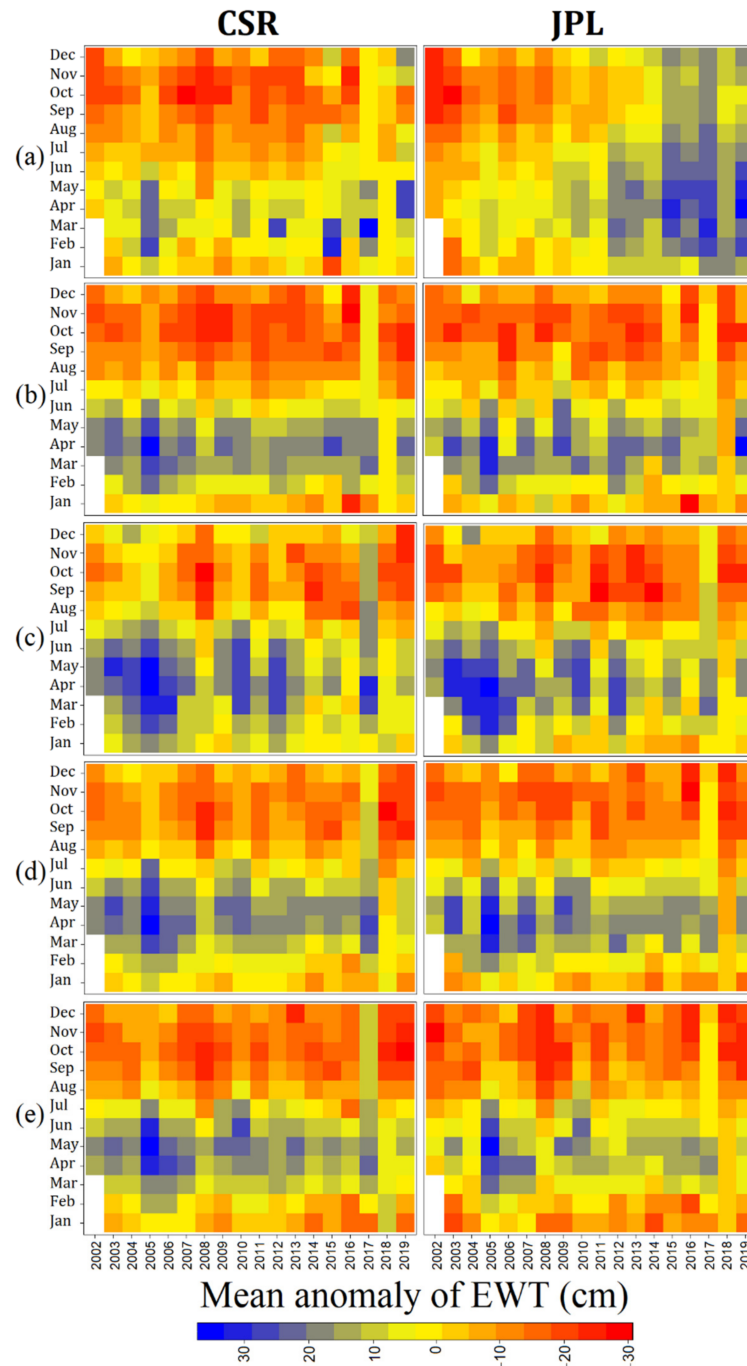


**Figure 2.** The monthly mean anomaly of EWT in (cm) at the five climate zones (rows) of the study area, obtained by CSR and JPL datasets (columns). Row (**a**) cold desert, (**b**) cold semi-arid (steppe), (**c**) hot-summer Mediterranean, (**d**) warm dry summer continental and (**e**) tundra.

### 4.2. Spatial Distribution of EWT

The standard deviation of EWT was calculated to assess the variability of water availability at each GRACE point, as shown in Figure 3. The variability in EWT was in the range of 0.65 to 38.06 cm for both the CSR and JPL. A higher value indicates less reliability

in water resources and vice versa. The figure shows higher variability (>30 cm) in the eastern and southeastern parts. It happened mainly in the tundra and warm dry continental climate. The variability decreases gradually toward the hot-summer Mediterranean climate zone. The variability was less or close to zero in the west and northwest of the basin. It means the reliability of water resources increases from hot-summer Mediterranean climate to cold semi-arid (steppe) and even cold desert climate zone. The result is consistent with that obtained by analyzing the monthly anomaly of EWT data presented in Figure 2.
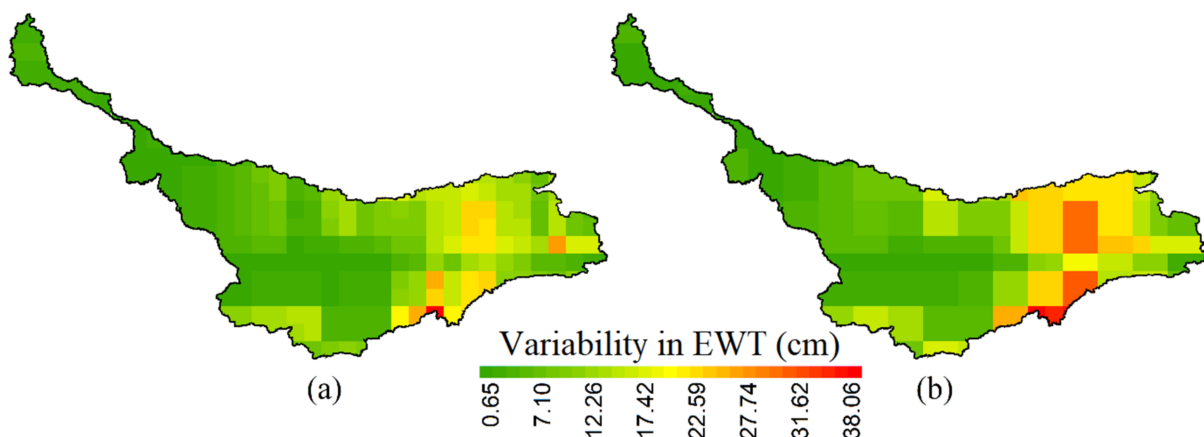


**Figure 3.** Variability of EWT (cm) in the basin for two GRACE products: (**a**) CSR and (**b**) JPL.

### 4.3. Trend Analysis of EWT

The spatial distributions of trends in annual average EWT for the CSR and JPL are shown in Figure 4. The rate of change in EWT is presented using a color ramp. The dots in the map indicate significant change at a 95% confidence interval. The rate of EWT change over the region was in the range from 0.08 to −0.12 cm/year. The figures indicate that EWT decreased during 2002–2019 in most parts of the basin's northeast, the tundra and warm dry continental climate zones. In contrast, a significant increase in EWT was noticed over major parts of the cold desert climate zone. This finding is consistent with that obtained through analysis of the monthly anomaly of EWT data presented in Figure 2.
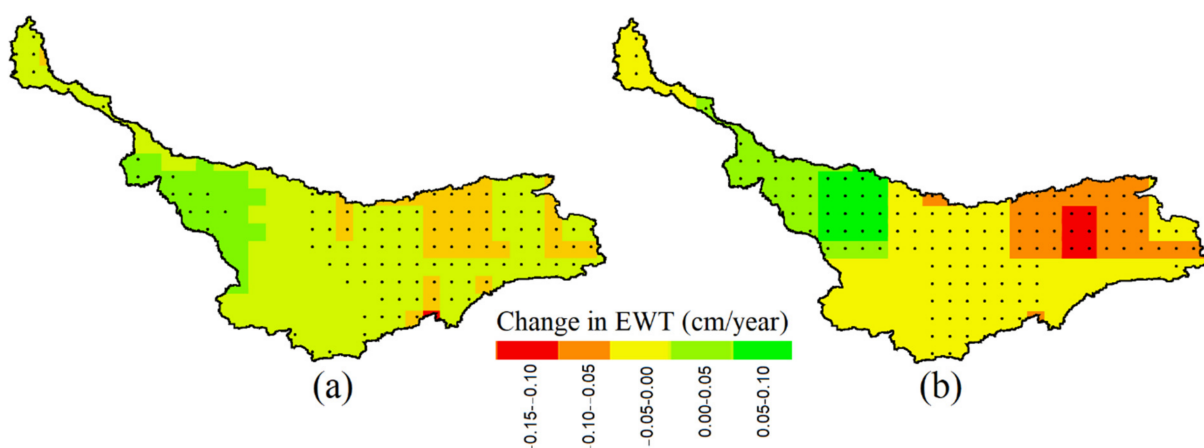


**Figure 4.** The spatial patterns of change in EWT (cm/year) for (**a**) CSR and (**b**) JPL. The color ramps show the rate of change obtained by applying Sen's slop, and the black dot inside each cell specifies the trend is significant at a 95% confidence interval obtained by MMK.

The study showed a higher decrease in the JPL EWT than the CSR, particularly in the tundra region in the northeast. The JPL EWT also showed a higher rising trend in water availability in the northwestern cold desert region than the CSR. The GRACE mascon

estimates EWT without considering the Earth's non-elastic processes [73]. Therefore, EWT trends are overestimated by mascon JPL, particularly in a glacial environment [74].

### 4.4. Spatial Distribution of Water Sustainability

The spatial distribution of water sustainability with its functions, reliability, resiliency and vulnerability is shown in Figure 5. The indexes were scaled in the range of 0.0–1.0 for presentation. The blue color in the map represents the higher values of the indexes. Overall, the two products (CSR and JPL) showed good consistency in the geographical distribution of the indexes. The higher reliability in water was noticed in the west of the basin, covering most of the cold desert and cold semi-arid climate of Uzbekistan and Turkmenistan countries. The JPL estimated the mean reliability over the study area as 0.48 compared to 0.45 for the CSR.

Resiliency showed a similar pattern to reliability: high in the west of the basin and low in the east. Vulnerability was higher in some areas of the tundra and warm dry continental climate zones in the east of the basin, mostly located in Afghanistan and Tajikistan. The JPL showed higher vulnerability than the CSR. The mean vulnerability of the JPL was 0.24 compared to 0.19 for the CSR.

The sustainability maps showed a spatial pattern similar to reliability and resiliency. The water resource in the western part of the basin was more sustainable than other climatic zones of the catchment. A higher value covers a small part of Afghanistan, a large area of Turkmenistan and most parts of Uzbekistan. The JPL showed high sustainability over a bigger area than the CSR. The eastern part of the basin is less sustainable except for a small land in the vicinity of China. Overall, water resources in the warm dry continental climate, hot-summer Mediterranean climate and small tundra climate zones were less sustainable, and cold desert and cold semi-arid climate zones were more sustainable.

Overall, the JPL estimated higher reliability and vulnerability in the basin than the CSR. The JPL also estimated higher sustainability of water resources than the CSR. The difference in the products was due to the difference in the EWT estimation algorithm used. It is not possible to evaluate the relative performance of the sustainability index estimated using different GRACE products due to the unavailability of in situ water resources data. However, both products provided a similar spatial pattern of water sustainability. Therefore, the results can be used with confidence to understand the spatial variability of sustainability in the basin. However, water sustainability at a grid point based on index value should be interpreted with caution.

### 4.5. Relation of Water Sustainability with Land Use and Population

Figure 6 shows the study area's land use and land cover map, derived from Copernicus Global Land Service (CGLS). Croplands dominates the basin's middle and northern regions, and the built-up areas are in the middle regions. The most water is consumed in agriculture and urban areas. Therefore, less sustainability in water resources (Figure 5) was noticed in the regions dominated by croplands and urban regions. It indicates that higher exploitation of water has made the northern and central regions of the basin less sustainable to water resources. Several irrigation canals have been built in the center parts of the basin. The Karakum canal is the largest and most famous among others [75]. In addition, one of the tallest hydropower dams, Rogun [76], has been constructed in the south part of Tajikistan over the Vash river as the main tributary of the Amu Darya. These indicate increased water consumption in the basin's middle and northern regions.
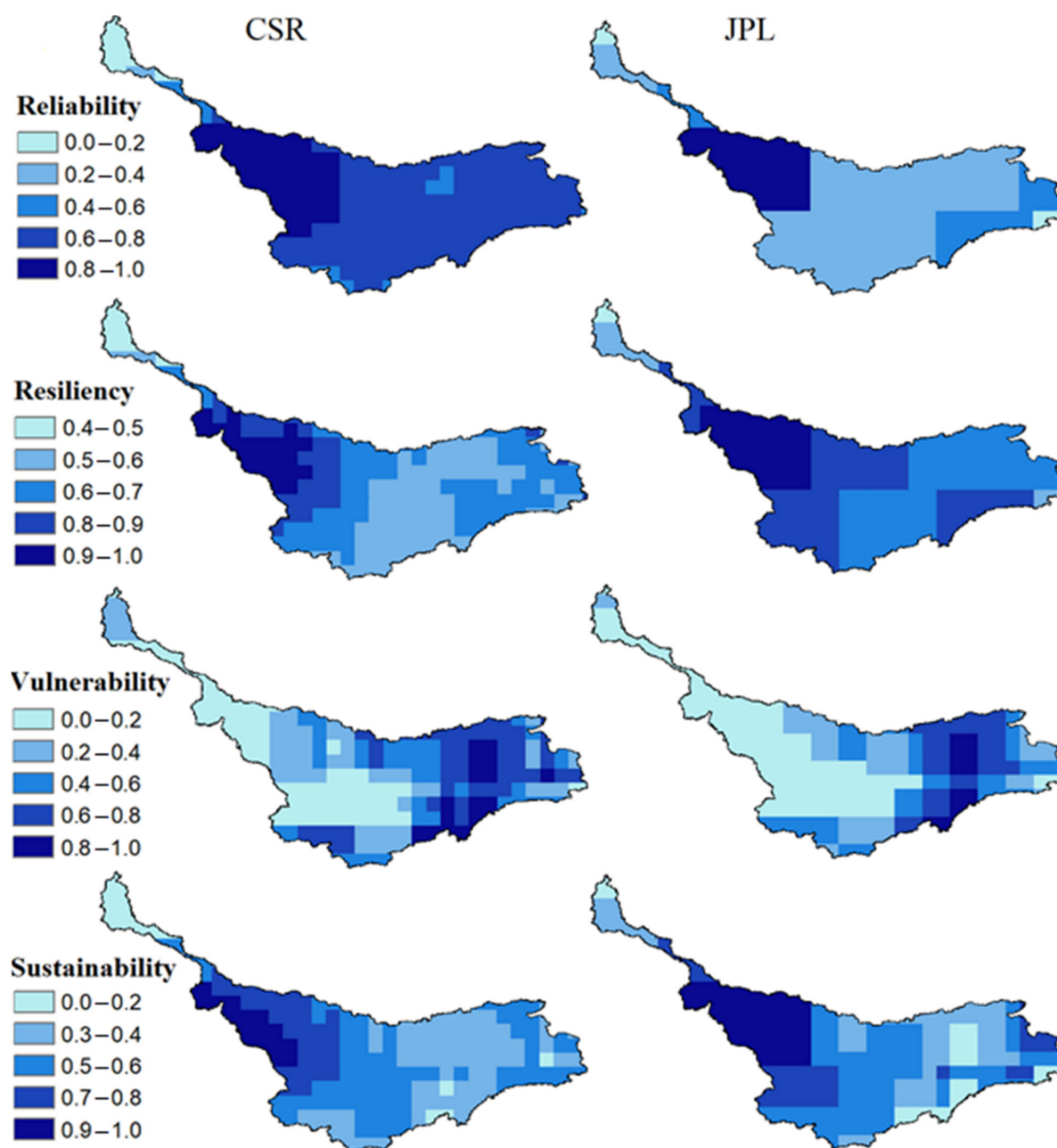
**Figure 5.** The spatial pattern of equivalent water thickness reliability, resiliency, vulnerability and sustainability (rows) using CSR and JPL GRACE solutions (columns).

The population density and the rate of change in population density are shown in Figure 7a,b. The figure shows a greater change in population density in the high-altitude southeast parts of the study area. The figure shows high population density in the central regions and small areas in the west and northwest, while the least population is in the eastern parts of the basin. Increased population density indicates a higher consumption of water. The least water sustainability in the basin (Figure 5) was noticed in the central-western part, where the population is increasing at the highest rate. Increasing population density also serves as a proxy of a region's growing economic activities and urbanization [77]. The water footprint is highly correlated to population density globally, indicating more water consumption in a more populated area [78]. Therefore, increasing population density indicates higher water consumption in some parts of the basin, making the water resources less sustainable in those regions.
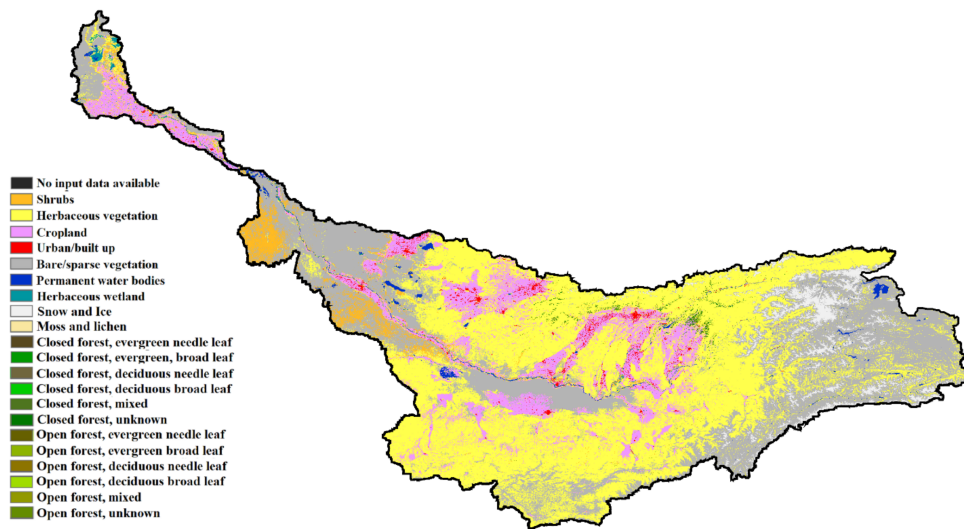
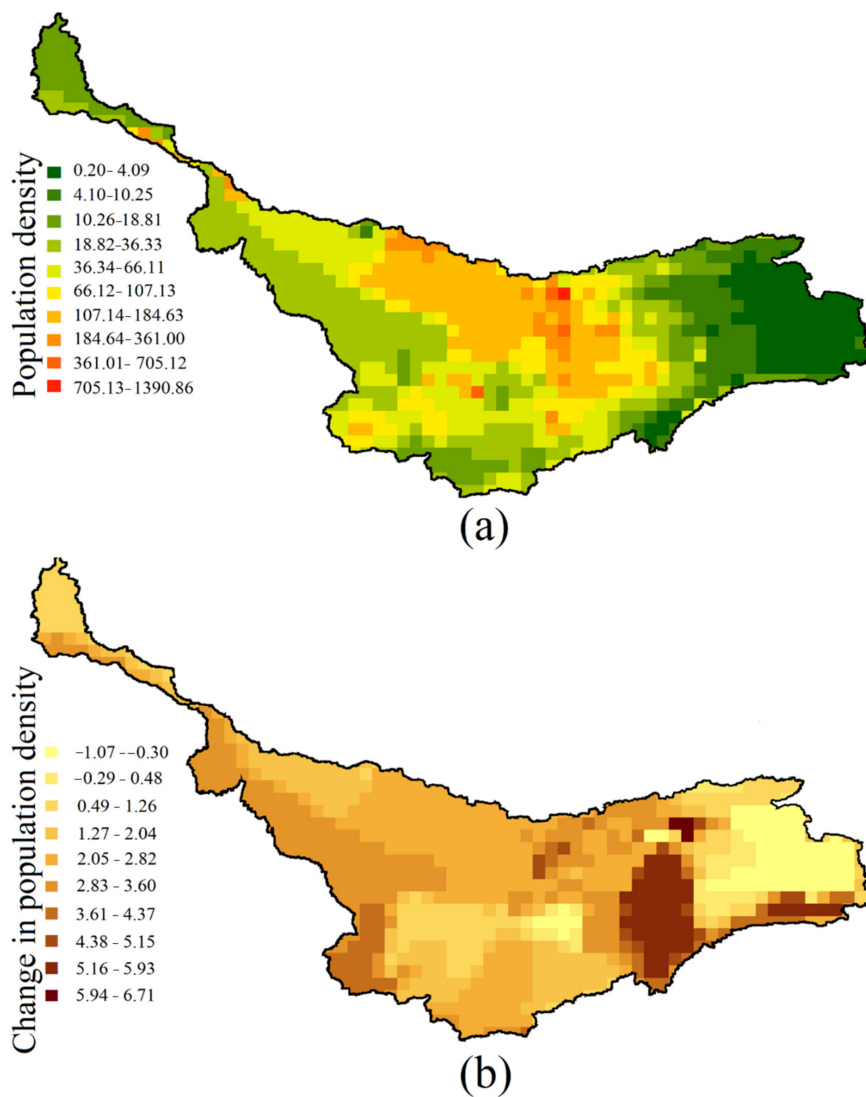**Figure 6.** Land use and land cover change over the study area for 2019.



**Figure 7.** (**a**) Population density (person/km2) in 2020; (**b**) rate of change in population density during 2000–2020.

## 5. Discussion

The monthly anomaly of GRACE solutions, including the CSR and the JPL after 2010, revealed a declining water shortage in all climatic zones, except in the cold desert climate, which shows an increase in water availability. The temporal variability of EWT (Figure 3) showed higher fluctuations in the east and a section in the central part of the study area, indicating a frequent disruption in water resources in these areas. However, water reliability was higher in the hot-summer Mediterranean and cold semi-arid (steppe) and cold desert climates.

The trend analysis (Figure 4) further supported the EWT anomaly and variability analysis results. The results show a decrease in water resources in the tundra and a small part in warm dry continental climate zones and the delta of the basin. In contrast, water resources in the Mediterranean climate, cold semi-arid (steppe) and most cold desert climate zones showed less variability.

Outcomes obtained using sustainability index components, including reliability and resiliency of EWT, showed more reliability and resiliency of water resources in cold semi-arid (steppe) climate and a part of the cold desert climate. In contrast, it was the opposite for the upstream regions of the basin covering tundra, warm dry continental and hot-summer Mediterranean climates. Spatial distribution of vulnerability was contrary to reliability and resiliency, showing the tundra and a part of warm dry continental climate zones are more vulnerable than the rest of the study area. Sustainability analysis of EWT, determined by combining resiliency, reliability and vulnerability, indicated the cold desert climate, cold semi-arid (steppe) and small areas of hot-summer Mediterranean climate are more sustainable in terms of water resources. Those regions cover a small part of Afghanistan, a major part of Turkmenistan and most of Uzbekistan. Water resources in some patches of tundra and warm dry continental climate zones of the basin covering a part of Afghanistan, Tajikistan and Kirgizstan are relatively less sustainable. The latter is constant with the research findings of Sediqi et al. [79] in some areas in the eastern part of the basin within the territory of Afghanistan. They also showed reasonable sustainability in water availability in the region. Salehie et al. [80] evaluated thermal bioclimate indicators (TBIs) in the Amu Darya river basin. Their results show a substantial rise in the diurnal temperature range (TBI2) in the eastern part of the basin in the tundra climatic zone. In addition, isothermality (TBI3) showed a greater increase in temperature in cold months than in warmer months in the same regions. This change in the climate of the upper east part of the basin could cause the melting of snow and glacier and the unsustainability of water in that area.

The gravity change data collected by the GRACE satellite is processed using the mass concentration block (mascon) algorithms to estimate EWT. The JPL and the CSR use different parameterizations in implementing the mascon algorithm [74]. The gravity analysis considers different Earth's processes, such as glacial isostatic tuning, elastic deformation, etc. The JPL and the CSR use different approaches for analysis which also causes a variation in EWT and the evaluation of water resources over a region [81]. Therefore, the present study also showed a difference in the EWT trend and variability and the difference indices estimated using the EWT.

The difference among GRACE EWT is often higher for the glacial environment [82]. The glacial isostatic adjustment is made in GRACE mascon products, assuming an elastic loading response of the solid Earth. Therefore, GRACE mascon products have been found suitable for estimating water resources of glacial catchments [74]. However, the JPL overestimates the variability and trends in EWT and thus the estimated indices using JPL EWT [74]. The present study also reported higher trends in JPL EWT and higher reliability and vulnerability estimated using JPL EWT.

It was not possible to evaluate the results obtained in this study due to the unavailability of in situ data of total water availability. The GRACE EWT products are prone to uncertainty due to parameterization of mascon algorithms, scale factors and measurement and leakage errors [81]. However, the two products used in this study provided a similar spatial pattern of water sustainability. Therefore, the spatial difference in water availability

can be accepted with confidence. However, grid-by-grid interpretation of the changes in water availability or water sustainability should be made with caution, as it is prone to high uncertainty. These points should be considered in water resources planning and management of the basin based on the results presented in this study.

## 6. Conclusions

The main goal of this study was to find out the availability and sustainability of water in the Amu Darya watershed by using GRACE data and employing the water sustainability index method. The findings indicate that the central part of the basin is more resilient and sustainable in terms of water availability. In contrast, the eastern region and delta of the basin are less resilient and more vulnerable. The high vulnerability of water in the upstream eastern section of the basin is probably due to significant changes in the climate in this region, as reported in several studies. Overall, the results of water availability using GRACE data by applying the water sustainability method were able to provide a better understanding of water resources availability of the basin. The maps created as part of this study have the potential to be used for water resources planning and development of the basin. In the future, the water sustainability map can be correlated with climate, land use and population distribution map to understand the driving factor of water sustainability in the basin. In addition, annual water sustainability can be estimated to understand its trends.

## References

1. Connor, R. *The United Nations World Water Development Report 2015: Water for a Sustainable World*; UNESCO publishing: Paris, France, 2015; Volume 1.
2. Sun, S.; Wang, Y.; Liu, J.; Cai, H.; Wu, P.; Geng, Q.; Xu, L. Sustainability assessment of regional water resources under the DPSIR framework. *J. Hydrol.* **2016**, *532*, 140–148. [CrossRef]
3. Hamed, M.M.; Nashwan, M.S.; Shahid, S.; Ismail, T. bin; Wang, X.; Dewan, A.; Asaduzzaman, M. Inconsistency in historical simulations and future projections of temperature and rainfall: A comparison of CMIP5 and CMIP6 models over Southeast Asia. *Atmos. Res.* **2022**, *265*, 105927. [CrossRef]
4. Hamed, M.M.; Nashwan, M.S.; Shahid, S. Intercomparison of Historical Simulation and Future Projection of Rainfall and Temperature by CMIP5 and CMIP6 GCMs Over Egypt. *Int. J. Climatol.* **2022**. [CrossRef]
5. Houmsi, M.R.; Shiru, M.S.; Nashwan, M.S.; Ahmed, K.; Ziarh, G.F.; Shahid, S.; Chung, E.S.; Kim, S. Spatial shift of aridity and its impact on land use of Syria. *Sustainability* **2019**, *11*, 7047. [CrossRef]
6. Hamed, M.M.; Nashwan, M.S.; Shahid, S. Performance Evaluation of Reanalysis Precipitation Products in Egypt using Fuzzy Entropy Time Series Similarity Analysis. *Int. J. Climatol.* **2021**, *41*, 5431–5446. [CrossRef]
7. Hamed, M.M.; Nashwan, M.S.; Shahid, S. A Novel Selection Method of CIMP6 GCMs for Robust Climate Projection. *Int. J. Climatol.* **2022**. [CrossRef]

8.    Shiru, M.S.; Shahid, S.; Chung, E.-S.; Alias, N. Changing characteristics of meteorological droughts in Nigeria during 1901–2010. *Atmos. Res.* **2019**, *223*, 60–73. [CrossRef]

9.    Pour, S.H.; Wahab, A.K.A.; Shahid, S.; Asaduzzaman, M.; Dewan, A. Low impact development techniques to mitigate the impacts of climate-change-induced urban floods: Current trends, issues and challenges. *Sustain. Cities Soc.* **2020**, *62*, 102373. [CrossRef]

10.   Ahmed, K.; Shahid, S.; Wang, X.; Nawaz, N.; Khan, N. Spatiotemporal changes in aridity of Pakistan during 1901–2016. *Hydrol. Earth Syst. Sci.* **2019**, *23*, 3081–3096. [CrossRef]

11.   Nashwan, M.S.; Shahid, S.; Wang, X. Assessment of satellite-based precipitation measurement products over the hot desert climate of Egypt. *Remote Sens.* **2019**, *11*, 555. [CrossRef]

12.   Salman, S.A.; Shahid, S.; Afan, H.A.; Shiru, M.S.; Al-Ansari, N.; Yaseen, Z.M. Changes in climatic water availability and crop water demand for Iraq region. *Sustainability* **2020**, *12*, 3437. [CrossRef]

13.   Ahmed, K.; Shahid, S.; Ali, R.O.; Harun, S. Bin; Wang, X.J. Evaluation of the performance of gridded precipitation products over balochistan province, pakistan. *Desalin. Water Treat.* **2017**, *79*, 73–86. [CrossRef]

14.   Flörke, M.; Schneider, C.; McDonald, R.I. Water competition between cities and agriculture driven by climate change and urban growth. *Nat. Sustain.* **2018**, *1*, 51–58. [CrossRef]

15.   Mehran, A.; AghaKouchak, A.; Nakhjiri, N.; Stewardson, M.J.; Peel, M.C.; Phillips, T.J.; Ravalico, J.K. Compounding impacts of human-induced water stress and climate change on water availability. *Sci. Rep.* **2017**, *7*, 6282. [CrossRef]

16.   Wada, Y.; Flörke, M.; Hanasaki, N.; Eisner, S.; Fischer, G.; Tramberend, S.; Ringler, C. Modeling global water use for the 21st century: The Water Futures and Solutions (WFaS) initiative and its approaches. *Geosci. Model. Dev.* **2016**, *9*, 175–222. [CrossRef]

17.   Boretti, A.; Rosa, L. Reassessing the projections of the world water development report. *NPJ Clean Water* **2019**, *2*, 15. [CrossRef]

18.   Rathnayaka, K.; Malano, H.; Arora, M. Assessment of sustainability of urban water supply and demand management options: A comprehensive approach. *Water* **2016**, *8*, 595. [CrossRef]

19.   Padowski, J.C.; Jawitz, J.W. Water availability and vulnerability of 225 large cities in the United States. *Water Resour. Res.* **2012**, *48*. [CrossRef]

20.   Mirrah, A.; Kusratmoko, E. Application of GIS for Assessment of Water Availability in the Cianten Watershed, West Java. In Proceedings of the 5th Geoinformation Science Symposium 2017 (GSS 2017), Yogyakarta, Indonesia, 27–28 September 2017.

21.   Maliehe, M.; Mulungu, D.M. Assessment of water availability for competing uses using SWAT and WEAP in South Phuthiatsana catchment, Lesotho. *Phys. Chem. EarthParts A/B/C* **2017**, *100*, 305–316. [CrossRef]

22.   Barlow, P.M.; Alley, W.M.; Myers, D.N. Hydrologic aspects of water sustainability and their relation to a national assessment of water availability and use. *Water Resour. Updat.* **2004**, *127*, 76–86.

23.   Maiolo, M.; Pantusa, D. Sustainable water management index, SWaM_Index. *Cogent Eng.* **2019**, *6*, 1603817. [CrossRef]

24.   Sandoval-Solis, S.; McKinney, D.; Loucks, D.P. Sustainability index for water resources planning and management. *J. Water Resour. Plan. Manag.* **2011**, *137*, 381–390. [CrossRef]

25.   Loucks, D.P. Quantifying trends in system sustainability. *Hydrol. Sci. J.* **1997**, *42*, 513–530. [CrossRef]

26.   Prakash, S.; Gairola, R.; Papa, F.; Mitra, A. An assessment of terrestrial water storage, rainfall and river discharge over Northern India from satellite data. *Curr. Sci.* **2014**, 1582–1586.

27.   Yin, W.; Hu, L.; Zhang, M.; Wang, J.; Han, S.C. Statistical Downscaling of GRACE-Derived Groundwater Storage Using ET Data in the North China Plain. *J. Geophys. Res. Atmos.* **2018**, *123*, 5973–5987. [CrossRef]

28.   Zhang, K.; Xie, X.; Zhu, B.; Meng, S.; Yao, Y. Unexpected groundwater recovery with decreasing agricultural irrigation in the Yellow River Basin. *Agric. Water Manag.* **2019**, *213*, 858–867. [CrossRef]

29.   Richey, A.S.; Thomas, B.F.; Lo, M.-H.; Reager, J.T.; Famiglietti, J.S.; Voss, K.; Swenson, S.; Rodell, M. Quantifying renewable groundwater stress with GRACE. *Water Resour. Res.* **2015**, *51*, 5217–5238. [CrossRef]

30.   Pang, Y.; Wu, B.; Cao, Y.; Jia, X. Spatiotemporal changes in terrestrial water storage in the Beijing-Tianjin Sandstorm Source Region from GRACE satellites. *Int. Soil Water Conserv. Res.* **2020**, *8*, 295–307. [CrossRef]

31.   Tapley, B.D.; Bettadpur, S.; Watkins, M.; Reigber, C. The gravity recovery and climate experiment: Mission overview and early results. *Geophys. Res. Lett.* **2004**, *31*. [CrossRef]

32.   Long, D.; Yang, Y.; Wada, Y.; Hong, Y.; Liang, W.; Chen, Y.; Chen, L. Deriving scaling factors using a global hydrological model to restore GRACE total water storage changes for China's Yangtze River Basin. *Remote Sens. Environ.* **2015**, *168*, 177–193. [CrossRef]

33.   Dai, C.; Shum, C.; Wang, R.; Wang, L.; Guo, J.; Shang, K.; Tapley, B. Improved constraints on seismic source parameters of the 2011 Tohoku earthquake from GRACE gravity and gravity gradient changes. *Geophys. Res. Lett.* **2014**, *41*, 1929–1936. [CrossRef]

34.   Wang, X.; Linage, C.; Famiglietti, J.; Zender, C.S. Gravity Recovery and Climate Experiment (GRACE) detection of water storage changes in the Three Gorges Reservoir of China and comparison with in situ measurements. *Water Resour. Res.* **2011**, *47*, W12502. [CrossRef]

35.   Mo, X.; Wu, J.; Wang, Q.; Zhou, H. Variations in water storage in China over recent decades from GRACE observations and GLDAS. *Nat. Hazards Earth Syst. Sci.* **2016**, *16*, 469–482. [CrossRef]

36.   Shamsudduha, M.; Taylor, R.G.; Jones, D.; Longuevergne, L.; Owor, M.; Tindimugaya, C. Recent changes in terrestrial water storage in the Upper Nile Basin: An evaluation of commonly used gridded GRACE products. *Hydrol. Earth Syst. Sci.* **2017**, *21*, 4533–4549. [CrossRef]

37.   Li, T.; Zhang, Q.; Zhao, Y.; Gao, Y. Detection of groundwater storage variability based on GRACE and CABLE model in the Murray-Darling Basin. *E3S Web Conf.* **2019**, *131*, 1067. [CrossRef]

38. Boergens, E.; Güntner, A.; Dobslaw, H.; Dahle, C. Quantifying the Central European droughts in 2018 and 2019 with GRACE Follow-On. *Geophys. Res. Lett.* **2020**, *47*, e2020GL087285. [CrossRef]

39. Cammalleri, C.; Barbosa, P.; Vogt, J. V Analysing the relationship between multiple-timescale SPI and GRACE terrestrial water storage in the framework of drought monitoring. *Water* **2019**, *11*, 1672. [CrossRef]

40. Jin, S.; Zhang, T. Terrestrial water storage anomalies associated with drought in southwestern USA from GPS observations. *Surv. Geophys.* **2016**, *37*, 1139–1156. [CrossRef]

41. Singh, A.; Reager, J.T.; Behrangi, A. Estimation of hydrological drought recovery based on precipitation and Gravity Recovery and Climate Experiment (GRACE) water storage deficit. *Hydrol. Earth Syst. Sci.* **2021**, *25*, 511–526. [CrossRef]

42. Qutbudin, I.; Shiru, M.S.; Sharafati, A.; Ahmed, K.; Al-Ansari, N.; Yaseen, Z.M.; Shahid, S.; Wang, X. Seasonal drought pattern changes due to climate variability: Case study in Afghanistan. *Water* **2019**, *11*, 1096. [CrossRef]

43. Pour, S.H.; Wahab, A.K.A.; Shahid, S. Spatiotemporal changes in aridity and the shift of drylands in Iran. *Atmos. Res.* **2020**, *233*, 104704. [CrossRef]

44. Unger-Shayesteh, K.; Vorogushyn, S.; Farinotti, D.; Gafurov, A.; Duethmann, D.; Mandychev, A.; Merz, B. What do we know about past changes in the water cycle of Central Asian headwaters? *A review. Glob. Planet. Chang.* **2013**, *110*, 4–25. [CrossRef]

45. Babow, S.; Meisen, P. *The Water-Energy Nexus in the Amu Darya River Basin: The Need for Sustainable Solutions to a Regional Problem*; Global Energy Network Institute: San Diego, CA, USA, 2012.

46. Khamzayeva, A.; Rahimov, S.; Islamov, U.; Maksudov, F.; Maksudova, D.; Sakiev, B. *Water Resources Management in Central Asia: Regional and International Issues at Stake*; CIDOB edicions: Barcelona, Spain, 2009.

47. Lioubimtseva, E. *Impact of Climate Change on the Aral Sea and its basin The Aral Sea*; Springer: Berlin/Heidelberg, Germany, 2014.

48. Glantz, M.H. Water, climate, and development issues in the Amu Darya Basin. *Mitig. Adapt. Strat. Glob. Chang.* **2005**, *10*, 23–50. [CrossRef]

49. Kure, S.; Jang, S.; Ohara, N.; Kavvas, M.L.; Chen, Z.Q. Hydrologic impact of regional climate change for the snowfed and glacierfed river basins in the Republic of Tajikistan: Hydrological response of flow to climate change. *Hydrol. Process.* **2013**, *27*, 4057–4070. [CrossRef]

50. Novikov, V.; Simonett, O.; Beilstein, M.; Bournay, E.; Berthiaume, C.; Kirby, A.; Rajabov, I. *Climate change in Central Asia—A Visual Synthesis*; Swiss Federal Office for the environment (FOEN), Zoı Environment Network: Vernier, Switzerland, 2009.

51. Jalilov, S.-M.; Keskinen, M.; Varis, O.; Amer, S.; Ward, F.A. Managing the water–energy–food nexus: Gains and losses from new water development in Amu Darya River Basin. *J. Hydrol.* **2016**, *539*, 648–661. [CrossRef]

52. Dodson, J.; Betts, A.V.; Amirov, S.; Yagodin, V.N. The nature of fluctuating lakes in the southern Amu-dar'ya delta. *Palaeogeogr. Palaeoclimatol. Palaeoecol.* **2015**, *437*, 63–73. [CrossRef]

53. Lutz, A.F.; Droogers, P.; Immerzeel, W. Climate change impact and adaptation on the water resources in the Amu Darya and Syr Darya River basins. *Rep. Futur.* **2012**, *110*, 1–116.

54. Hagg, W.; Hoelzle, M.; Wagner, S.; Mayr, E.; Klose, Z. Glacier and runoff changes in the Rukhk catchment, upper Amu-Darya basin until 2050. *Glob. Planet. Chang.* **2013**, *110*, 62–73. [CrossRef]

55. White, C.J.; Tanton, T.W.; Rycroft, D.W. The impact of climate change on the water resources of the Amu Darya Basin in Central Asia. *Water Resour. Manag.* **2014**, *28*, 5267–5281. [CrossRef]

56. Immerzeel, W.; Lutz, A.; Droogers, P. *Climate Change Impacts on the Upstream Water Resources of the Amu and Syr Darya River Basins*; FutureWater: Wageningen, The Netherlands, 2012.

57. Nezlin, N.P.; Kostianoy, A.G.; Lebedev, S.A. Interannual variations of the discharge of Amu Darya and Syr Darya estimated from global atmospheric precipitation. *J. Mar. Syst.* **2004**, *47*, 67–75. [CrossRef]

58. Wegerich, K. Hydro-hegemony in the Amu Darya basin. *Water Policy* **2008**, *10*, 71–88. [CrossRef]

59. Kumar, N.; Khamzina, A.; Tischbein, B.; Knöfel, P.; Conrad, C.; Lamers, J.P. Spatio-temporal supply–demand of surface water for agroforestry planning in saline landscape of the lower Amudarya Basin. *J. Arid Environ.* **2019**, *162*, 53–61. [CrossRef]

60. Crosa, G.; Froebrich, J.; Nikolayenko, V.; Stefani, F.; Galli, P.; Calamari, D. Spatial and seasonal variations in the water quality of the Amu Darya River (Central Asia). *Water Res.* **2006**, *40*, 2237–2245. [CrossRef] [PubMed]

61. Schlüter, M.; Savitsky, A.G.; McKinney, D.C.; Lieth, H. Optimizing long-term water allocation in the Amudarya River delta: A water management model for ecological impact assessment. *Environ. Model. Softw.* **2005**, *20*, 529–545. [CrossRef]

62. Sun, J.; Li, Y.; Suo, C.; Liu, Y. Impacts of irrigation efficiency on agricultural water-land nexus system management under multiple uncertainties—A case study in Amu Darya River basin, Central Asia. *Agric. Water Manag.* **2019**, *216*, 76–88. [CrossRef]

63. Schlüter, M.; Khasankhanova, G.; Talskikh, V.; Taryannikova, R.; Agaltseva, N.; Joldasova, I.; Abdullaev, U. Enhancing resilience to water flow uncertainty by integrating environmental flows into water management in the Amudarya River, Central Asia. *Glob. Planet. Chang.* **2013**, *110*, 114–129. [CrossRef]

64. Ahmad, M.; Wasiq, M. *Water Resource Development in Northern Afganistan and Its Implications for Amu Darya Basin: The World Bank*; World Bank Publications: Washington, DC, USA, 2004; ISBN 0821358901.

65. Normatov, P.I.; Normatov, I.S. Monitoring of Meteorological, Hydrological Conditions and Water Quality of the Main Tributaries of the Transboundary Amu Darya River. In *Achievements and Challenges of Integrated River Basin*; IntechOpen: London, UK, 2018.

66. Jalilov, S.-M.; Amer, S.A.; Ward, F.A. Reducing conflict in development and allocation of transboundary rivers. *Eurasian Geogr. Econ.* **2013**, *54*, 78–109. [CrossRef]

67. Behzod, G.; Su-Chin, C. Water salinity changes of the gauging stations along the Amu Darya River. *J. Agric. For.* **2013**, *62*, 1–14.

68. Wang, X.; Luo, Y.; Sun, L.; He, C.; Zhang, Y.; Liu, S. Attribution of runoff decline in the Amu Darya River in Central Asia during 1951–2007. *J. Hydrometeorol.* **2016**, *17*, 1543–1560. [CrossRef]

69. Hirsch, R.M.; Slack, J.R. A nonparametric trend test for seasonal data with serial dependence. *Water Resour. Res.* **1984**, *20*, 727–732. [CrossRef]

70. McLeod, A.I.; Hipel, K.W. Simulation procedures for Box-Jenkins models. *Water Resour. Res.* **1978**, *14*, 969–975. [CrossRef]

71. Asefa, T.; Clayton, J.; Adams, A.; Anderson, D. Performance evaluation of a water resources system under varying climatic conditions: Reliability, Resilience, Vulnerability and beyond. *J. Hydrol.* **2014**, *508*, 53–65. [CrossRef]

72. Hashimoto, T.; Stedinger, J.R.; Loucks, D.P. Reliability, resiliency, and vulnerability criteria for water resource system performance evaluation. *Water Resour. Res.* **1982**, *18*, 14–20. [CrossRef]

73. Sun, Y.; Riva, R.E.M. A global semi-empirical glacial isostatic adjustment (GIA) model based on Gravity Recovery and Climate Experiment (GRACE) data. *Earth Syst. Dyn.* **2020**, *11*, 129–137. [CrossRef]

74. Jing, W.; Zhang, P.; Zhao, X. A comparison of different GRACE solutions in terrestrial water storage trend estimation over Tibetan Plateau. *Sci. Rep.* **2019**, *9*, 1765. [CrossRef] [PubMed]

75. Brite, E.B. The hydrosocial empire: The Karakum River and the Soviet conquest of Central Asia in the 20th century. *J. Anthropol. Archaeol.* **2018**, *52*, 123–136. [CrossRef]

76. Havenith, H.-B.; Torgoev, I.; Ischuk, A. Integrated geophysical-geological 3D model of the right-bank slope downstream from the Rogun dam construction site, Tajikistan. *Int. J. Geophys.* **2018**, *2018*, 1641789. [CrossRef]

77. Liu, G.; Hu, F.; Wang, Y.; Wang, H. Assessment of Lexicographic Minimax Allocations of Blue and Green Water Footprints in the Yangtze River Economic Belt Based on Land, Population, and Economy. *Int. J. Environ. Res. Public Health* **2019**, *16*, 643. [CrossRef] [PubMed]

78. Baker, R.J.; Scott, D.M.; King, P.J.; Overall, A.D.J. Genetic structure of regional water vole populations and footprints of reintroductions: A case study from southeast England. *Conserv. Genet.* **2020**, *21*, 531–546. [CrossRef]

79. Sediqi, M.N.; Shiru, M.S.; Nashwan, M.S.; Ali, R.; Abubaker, S.; Wang, X.; Ahmed, K.; Shahid, S.; Asaduzzaman, M.; Manawi, S.M.A. Spatio-temporal pattern in the changes in availability and sustainability of water resources in Afghanistan. *Sustainability* **2019**, *11*, 5836. [CrossRef]

80. Salehie, O.; Ismail, T.; Shahid, S.; Sammen, S.S.; Malik, A.; Wang, X. Selection of the Gridded Temperature Dataset for Assessment of Thermal Bioclimatic Environment Changes in Amu Darya River Basin. *Res. Sq.* 2021. [CrossRef]

81. Seyoum, W.M.; Kwon, D.; Milewski, A.M. Downscaling GRACE TWSA Data into High-Resolution Groundwater Level Anomaly Using Machine Learning-Based Models in a Glacial Aquifer System. *Remote Sens.* **2019**, *11*, 824. [CrossRef]

82. Jin, S.; Zhang, T.Y.; Zou, F. Glacial density and GIA in Alaska estimated from ICESat, GPS and GRACE measurements. *J. Geophys. Res. Earth Surf.* **2017**, *122*, 76–90. [CrossRef]